International Soil and Water Conservation Research 13 (2025) 795–807

Contents lists available at ScienceDirect

International Soil and Water Conservation Research

journal homepage: www.elsevier.com/locate/iswcr

Original Research Article

Fingerprinting using compound-specific $\delta^{13}C$ of n-alkanes reveals the temporary role of paddy fields as a secondary source for watershed sediment loss

Qiang Tang [a,*], Fangxin Chen [b], Guangyu Zhu [c], Xiubin He [d], Jie Wei [e], Yusheng Zhang [f], Hari Ram Upadhayay [f], Adrian Joynes [f], Adrian L. Collins [f]

[a] Chongqing Jinfo Mountain Karst Ecosystem National Observation and Research Station, School of Geographical Sciences, Southwest University, Chongqing, 400715, China
[b] College of Resources and Environment, Southwest University, Chongqing, 400715, China
[c] College of Environment and Ecology, Chongqing University, Chongqing, 400044, China
[d] Key Laboratory of Mountain Surface Processes and Ecological Regulation, Institute of Mountain Hazards and Environment, Chinese Academy of Sciences, Chengdu, 610299, China
[e] School of Geography and Tourism, Chongqing Normal University, Chongqing, 401331, China
[f] Net Zero and Resilient Farming, Rothamsted Research, North Wyke, Okehampton, Devon, EX20 2SB, UK

ARTICLE INFO

Article history:
Received 22 August 2024
Received in revised form
13 June 2025
Accepted 9 July 2025
Available online 9 July 2025

Keywords:
Sediment source fingerprinting
Biomarkers
Compound-specific $\delta^{13}C$
n-alkanes
Bayesian mixing model

ABSTRACT

Fingerprinting generates reliable sediment provenance information which supports devising policy or practical strategies for soil conservation and sediment management, but it remains challenging in areas with fragmented landscapes and diverse land use practices. This study evaluated the seasonality of biomarker signatures and their variability among particle size fractions, and apportioned target time-integrated suspended sediment to land use-based sources in an intensive agricultural watershed with mosaic land use patch configurations and crop-specific farming practices. Source materials (i.e., topsoil) from dry croplands, paddy fields and citrus orchards were sampled, and target time-integrated suspended sediment samples were collected at the watershed outlet. The content and compound-specific $\delta^{13}C$ of long-chain saturated n-alkanes (C_{23}-C_{33}) were determined for two particle size fractions (i.e., <25 μm, 25–63 μm). The $\delta^{13}C$ of monomeric n-alkanes displayed insignificant variabilities between particle size fractions and temporal variability across the sampling period. The MixSIAR Bayesian model was employed to quantify sediment source contributions. Due to land disturbance by tillage and crop plantation, our results revealed that paddy fields act as an important temporary secondary sediment source despite such fields conventionally being recognized as sediment sinks. Regardless, dry farmland remains the largest contributor to watershed sediment loss. A range of measures such as soil virginization, returning straw to fields, and pasture cultures in orchards are recommended for precision sediment management at watershed scale.

1. Introduction

The earth's soil denudation system has been severely disturbed by the expansion and intensification of human activities, such as large-scale deforestation, land clearance and reclamation, commercial farming, infrastructure construction, dam construction and reservoir impoundment, conservation practices, and urbanization (Jenny et al., 2019). Consequently, global soil erosion patterns have been unprecedently complicated over recent decades

* Corresponding author.No. 2, Tiansheng Road, Beibei District, Chongqing, 400715, China.
E-mail address: qiangtang@swu.edu.cn (Q. Tang).

Peer review under the responsibility of International Research and Training Center on Erosion and Sedimentation, the China Water & Power Press, and China Institute of Water Resources and Hydropower Research.

https://doi.org/10.1016/j.iswcr.2025.07.005

(Borrelli et al., 2020; Wuepper et al., 2020). Suspended sediment generated by the mobilization of eroded materials from distal uplands or proximal within-channel sources acts as an essential structural and functional component of river channels (Apitz, 2012). Its transport dynamics determine the extent and intensity of geomorphological evolution (aggradation or degradation) of fluvial channels and modulates the continent-ocean delivery of terrestrial materials (Ludwig et al., 1996; Walling, 2006). More recently, growing awareness has been directed to the ecological significance of suspended sediment in rivers since fine-grained particles represent a key vector for contaminants (e.g., nutrients, carbon, inorganic elements, and organic compounds, etc.) redistribution, which deliver detrimental consequences to water quality and river ecology more generally (Walling & Fang, 2003).

Acquiring reliable sediment source information in catchments is critical in devising policies or measures for soil conservation and sediment management, but it remains challenging given the diffuse nature of sediment mobilization and redistribution, and their concomitant variability in space and time. Sediment source fingerprinting provides a useful alternative to quantify the relative contributions of sources to target sediments via establishing a direct fingerprint link of tracer signatures between source and target sediment (Collins & Walling, 2004). Its applicability across landscapes with contrasting environmental contexts has been improved through the use of an increasing number of tracers represented by inherent soil properties, such as physical properties (Martinez-Carreras et al., 2010; Pulley et al., 2018), fallout radionuclides (Pulley et al., 2019), mineral magnetisms (Kayvantash et al., 2017; Rowntree et al., 2017), stable isotopes (Fox & Papanicolaou, 2008; Mabit et al., 2018), geochemical elements (Chen et al., 2019), optical tracers (Tiecher et al., 2016; Verheyen et al., 2014), and biomarkers (Blake et al., 2012; Chen et al., 2017; Hancock & Revill, 2013). More recently, compound-specific stable isotopes have been increasingly employed given its potential to apportion land use-based sources. A premise, here, lies in the fact that land use or vegetation cover can imprint soil with a specific $\delta^{13}C$ signature through organic matter inputs (Upadhayay et al., 2017). Biomarkers, including for example, long-chain saturated n-alkanes with a strong odd/even predominance derived from terrestrial higher plants, are found to be highly resistant to microbial decomposition and persist in the environment in conjunction with sediment mobilization and storage (Blake et al., 2012; Cooper et al., 2015). Here, however, as landscape fragmentation can potentially result in greater within-source variability of tracer signatures, the diagnostic power of biomarkers needs to be evaluated carefully (Reiffarth et al., 2019; Upadhayay, Lamichhane, et al., 2020).

Equally, the temporal coverage and resolution is flexible when using a variety of targeted sediment sampling strategies including, for example, snapshot suspended sediment sampling throughout the hydrographs of individual rainfall events, time-integrated suspended sediment sampling, channel bed sediment remobilization or the coring of floodplain deposits (Owens et al., 1999), or historical sedimentary archives preserved in lakes or reservoirs (Ben Slimane et al., 2013; Fang, 2015; Huang et al., 2019; Kim et al., 2013). The most recent work has revisited major technological assumptions;, for example, reexamining the conservative behaviour or diagnostic ability of both traditional and novel tracers by evaluating the spatial and temporal within-source variability of tracer signatures (Collins et al., 2019; Du & Walling, 2017; Reiffarth et al., 2016), or testing the appropriateness of conventional source classification schemes and providing methodologies for refining source classification strategies (Pulley et al., 2017; Vercruysse & Grabowski, 2018; Zhou et al., 2016). Fingerprint tracers are chosen according to the physical context of the research catchment in question (e.g., different geologies, land uses, etc.). For example, in areas where lithology controls erosion, geochemical fingerprints are commonly used in sediment fingerprinting (Fox & Papanicolaou, 2008; Mabit et al., 2018; Martinez-Carreras et al., 2010; Pulley et al., 2019; Rowntree et al., 2017; Tiecher et al., 2016; Verheyen et al., 2014); whereas in situations where geological variations are small or where different land uses span geological boundaries, biomarkers are increasingly shortlisted as potentially useful fingerprint properties (Blake et al., 2012; Chen et al., 2017; Hancock & Revill, 2013; Mabit et al., 2018; Tiecher et al., 2016). The number and structures of un-mixing models for estimating source proportions has also expanded. Here, models are either frequentist or Bayesian but can also differ within either category with regards the inclusion or exclusion or various correction factors and weightings (Collins et al., 1997). Whereas as early studies typically used the <63 μm fraction regardless of catchment setting or tracer selection (Collins et al., 1997), it is now recommended that careful attention be directed towards adoption of the most relevant size fraction for both (Collins et al., 2017). In some cases, this has resulted in the use of the <10 μm fraction (Theuring et al., 2015).

Sediment fingerprinting has been mostly undertaken in homogeneous landscapes with larger field sizes and simple farming practices. But landscapes are heavily fragmented in the hilly and mountainous regions in China, characterized by mosaic land use patches under the household-based farming systems with diverse cropping selections and farming practices. Fragmented landscapes with complex land use patterns and histories potentially present a particular challenge to the capacity to identify and apply diagnostic source fingerprints (Tang et al., 2019). In addition, paddy fields represent a popular agricultural land use in southern China, which have been traditionally viewed as sediment sinks, but, from a longer-term perspective, could be a secondary sediment source given the remobilization of deposited sediment from previous rainfall events. In the specific case of testing biomarkers in such settings, two issues require further investigation. One is the comparison of biomarker source apportionment using different particle size fractions, and the other is whether biomarker signatures remain stable or conservative over the long-term (Chen et al., 2017; Hancock & Revill, 2013). To this end, this study attempts to examine the temporal variability of biomarker tracers (i.e., absolute abundance and $\delta^{13}C$ of n-alkanes) related to land use and vegetation cover and variability among different particle size fractions and to, and quantify the relative contributions of land use based source units to target time-integrated suspended sediments in a representative intensive farming watershed with fragmented landscape and dynamic agricultural land use in the Three Gorges Reservoir Area. This is an area where soil conservation is of utmost priority given its potential consequences for lowland reservoir sedimentation, water quality deterioration and aquatic ecosystem health. In particular, paddy fields were selected as a potential sediment source and their role in watershed sediment loss was quantified and explored.

2. Materials and methods

2.1. Site description

The Three Gorges Reservoir Area is located at the eastern edge of the Sichuan Depression in southwestern China (Fig. 1(a)). Regional landform is hilly and mountainous. The climate is dominated by humid temperate monsoons. Land use is highly related to topography and human occupation. Forests and grasslands prevail in the mountainous area where population density is low, while agricultural land is predominant in the hilly area with

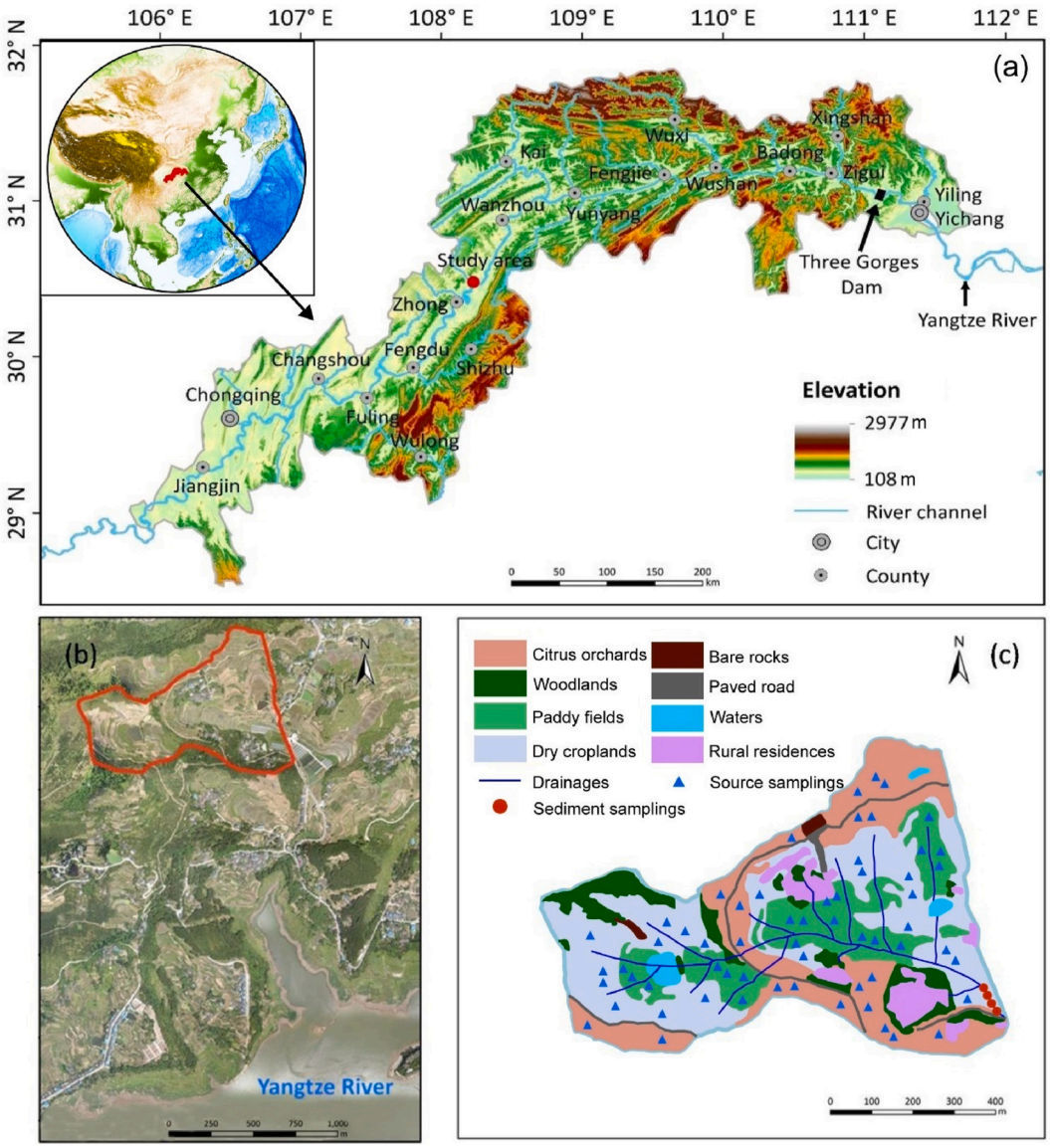

Fig. 1. (a): Map of the geographical context of the Three Gorges Reservoir Area; (b): Remote sensing image generated by a drone flying over the study watershed, and; (c): Land use of the study watershed.

high population density. Agriculture is managed by small-sized household crop farms in the form of dry croplands and paddy fields. Significant land use change has taken place due to dam construction, urbanization, infrastructure expansion, land abandonment, and a reforestation campaign, wherein arable lands were converted to woodlands, grasslands or urban areas. Human translocation and water impoundment increased regional land resource scarcity, leading to farming extension on marginal range lands and more intensive cultivation practices. This area has exhibited high rates of soil erosion, which threatens sustainable land productivity and the ecosystem health of lowland receiving waterbodies. Soil conservation is thus of high management priority to prevent the world's largest reservoir from rapid sedimentation and water quality deterioration from diffuse contaminant export (Fu et al., 2010).

This study was conducted in a small watershed (0.25 km^2) at Zhong County in the central Three Gorges Reservoir Area (Fig. 1 (b)). Its landform is hilly with elevations ranging from 209 to 322 m a.s.l. The purple soil, which is developed from the Triassic-Cretaceous system of sedimentary rocks and classified as Regosols in the FAO Taxonomy or Entisols in the USDA Taxonomy (He et al., 2009), is highly susceptible to rainfall detachment and runoff dispersal. Annual average rainfall is 1172 mm and a major proportion occurs in the rainy season from May to September. Watershed-wide land use consists of dry croplands (36 %), citrus orchards (35 %), paddy fields (19 %), rural residences (5.7 %), paved roads (1.9 %), water (1.7 %) and exposed bare rock (0.7 %) (Fig. 1(c)). The uplands are predominantly occupied by sloping or terraced dry croplands (Fig. 2(a)) which are intensively cultivated throughout the year. Canola (*Brassica napus* L.) and cabbage (*Brassica oleracea* L. var. capitata L.) are major winter crops, while maize (*Zea mays* L.) and sweet potato (*Ipomoea batatas* (L.) Lam.) are major summer crops. Citrus orchards along the middle slopes were converted from dry croplands for more than 15 years (Fig. 2 (b)), which experience the least intensity of land disturbance as no tillage is practiced but receive large inputs of agricultural chemicals such as pesticides, herbicides, and fertilizers, and are therefore likely to be a high-risk source for diffuse pollution generation.

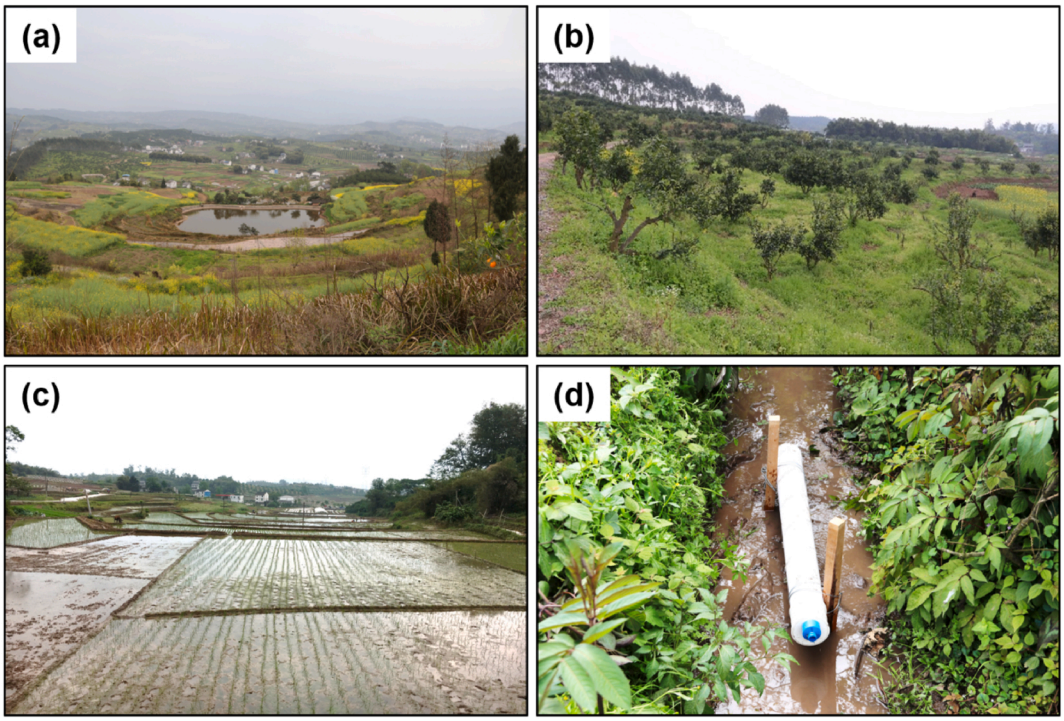

Fig. 2. Photographs of the study watershed. (a): dry croplands; (b): Citrus orchards converted from dry croplands for more than 15 years; (c): paddy fields at the end of April, showing a low water level meaning that the soil disturbed by mechanical ploughing is prone to erosion; and; (d): time-integrated suspended sediment sampler installed near the watershed outlet.

Paddy fields are distributed on the valley floors where rice is planted from April to August (Fig. 2(c)). These fields remain uncultivated and impounded with shallow water in the winter season but undergo mechanical tillage before rice reseeding in April.

2.2. Sampling strategies

Watershed generic sediment sources were classified *a priori* as dry croplands, citrus orchards, and paddy fields in our study. Mosaic bare rock, woodlands, rural residences, and paved roads were excluded from sediment sources given their relatively minor importance in soil erosion and sediment supply. Individual topsoil (0–2 cm) source samples were composed of 10 random subsamples collected in an immediate vicinity using a stainless-steel corer. Composite samples were collected to improve the spatial representativeness of source material samples across the watershed. Six composite topsoil samples were collected for each source category (18 source samples in total) in late March 2017 before the ploughing of the paddy fields and rice reseeding, while 14 composite topsoil samples were taken (42 source samples in total) in late April 2018 after paddy field ploughing and rice reseeding. Target time-integrated suspended sediment samples were collected using four independent Phillips samplers (Phillips et al., 2000) installed at the watershed outlet from March 2017 to September 2018 (Fig. 2(d)). Samplers were deployed in May 2017 during the first field campaign. The first sample retrieval was conducted in July 2017 when one composite sample was obtained by mixing four independent samples. During suspended sediment retrieval, large organic detritus was removed manually and sediment was settled in a dark cool room for 7–10 days. Excess water was siphoned off without disturbing the settled sediment. In total, nine samples were collected in 2017 and a further six samples in 2018 (Table 1).

2.3. Laboratory analysis

Both source and suspended sediment samples were freeze-dried, manually disaggregated, and sieved through a 63 μm mesh. To select the most appropriate particle size fraction for the source fingerprinting work, time-integrated suspended sediment samples were analyzed for absolute grain size with a Malvern Mastersizer laser diffraction granulometer, following pre-treatment with hydrogen peroxide and ultrasonic dispersion post the application of sodium hexametaphosphate as a dispersal agent. This analysis indicated that the d_{90} of the absolute particle size of the target time-integrated suspended sediment samples ranged from 41 to 60 μm, with a corresponding average of 48 μm and a median of 49 μm. Because it is also informative to consider any potential effects of tracer distribution within particle size fractions of source and target sediment samples, especially where the d_{90} is reasonably coarse, all samples were separated into <25 μm and 25–63 μm fractions. This provided a basis for comparing source fingerprinting results for two absolute particle size fractions.

Sample extraction and n-alkanes fractionation were performed using the following procedure. Approximately 10 g of sample was weighed into a thimble and soxhlet extracted with 250 ml of dichloromethane (DCM): acetone (9:1, v/v) for 24 h. Before the extraction, a 100 μl of 1 mg/ml C_{19} and C_{34} n-alkane internal standard was added. The total lipid extract (TLE) was evaporated to dryness using a rotatory evaporator (*Buchi*), then re-dissolved in 3 × 2 ml DCM: acetone (1:1), transferred to a vial and re-evaporated to dryness under a gentle stream of nitrogen (N_2) at 37 °C. To obtain a neutral lipid extract (NL), the TLE was dissolved in a ml of chloroform, the 0.5 ml of the extract was eluted through an activated silica column 60A, particle size 35–70, (Fisher Scientific), with 5 ml of chloroform and then blown down to dryness with N_2. To obtain the hydrocarbon fraction containing the n-

Table 1
Summary of field sampling scheme for prescribed sources and target time-integrated suspended sediments over 2017–2018.

Watershed-wide land use based sediment sources			Target time-integrated suspended sediment	Sampling time
Citrus orchards	Dry croplands	Paddy fields		
6	6	6		Mar 2017[a]
			1	Jul 2017[b]
			4	Aug 2017
			4	Oct 2017
14	14	14	4	Apr 2018[c]
			2	Sep 2018

[a] Source samples from paddy fields were taken before ploughing and rice reseeding, sediment samplers were installed during this field trip.
[b] One composite time-integrated sediment sample was obtained by mixing sediments collected from four independent samplers.
[c] Independent source samples from paddy fields were collected after ploughing and rice reseeding.

alkanes, the NL was dissolved in 2 ml hexane, 0.5 ml was eluted through another silica column with 4 ml of hexane and then blown down to dryness with N_2.

The absolute abundance of n-alkanes (C_{23-33}) was quantified using an Agilent 7890A GC with a flame ionization detector (FID), 7963 autosampler and splitless injector at 300 °C (Agilent Technologies). Prior to analysis, the hydrocarbon fraction was re-dissolved in 2 ml of hexane and 100 μl transferred to a 2 ml vial. The oven programme was hold at 40 °C for 1 min, then ramp to 130 °C at 20 °C per minute, then 4 °C per minute to 300 °C and hold for 10 min. The GC column was an Agilent HP-5 (30 m × 320 μm x 0.250 μm) with helium carrier gas at a flow rate of 1 ml per minute. The odd n-alkanes (C_{23}-C_{33}) were initially identified by retention times and distinctive odd/even patterns. The concentrations were determined relative to the C_{34} internal standard. The identity of the n-alkanes was confirmed using GC-MS. Here, the n-alkanes spectra were compared to those in the National Institute of Standards spectral library (NIST, US Gov.) and characteristic base peaks identified.

The compound-specific $\delta^{13}C$ signatures of n-alkanes ($\delta^{13}C_{23-33}$) were determined using a Finnigan Mat 6890 GC coupled to a Finnigan Mat Delta Plus IRMS via a Combustion III interface, with oxidation reactor containing platinum/copper oxide and nickel oxide at 940 °C (Thermo Fisher Scientific, Bremen, Germany). Samples were introduced using a PAL AS200 autosampler (CTC analytics, Switzerland) via splitless injector at 300 °C with helium carrier gas at 1.4 ml per minute. The oven programme was the same as above, but the column was a Varian CP-SIL 5CB (50 m × 320 μm x 0.12 μm) (Varian Inc. California, US). The $\delta^{13}C$ ratio was determined relative to CO_2 reference gas of known $\delta^{13}C$ and N5.5 grade purity (BOC, Guildford, UK) previously calibrated by Iso-Analytical. The reference gas was injected directly to the source just prior to the n-alkane peaks of interest, and four times at the beginning and end of each run. The $\delta^{13}C$ was expressed relative to Vienna Pee Dee Belemnite (VPDB). During the runs, the known $\delta^{13}C$ values of the C_{19} and C_{34} internal standard (determined in house) in the samples was monitored as well as running the n-alkane standards at the beginning and end of each batch. The operation of the system was regularly checked using a certified n-alkane compound mixture C_{16}-C_{30} (Indianna State University, US) with variable $\delta^{13}C$ values over a range of concentrations. The $\delta^{13}C$ should be > 1 ‰ from the reference value. The stability and linearity of the system were better than 0.06 ‰. The $\delta^{13}C$ standard deviation from the standards was ±0.35 ‰.

2.4. Sediment source fingerprinting procedure

Prior to un-mixing source contributions to the target time-integrated suspended sediments, tracer property conservation was assessed using a bracket test to ensure that sediment tracer signatures fall within the measured range for each source group. Selected conservative tracers were then tested individually for their source discrimination efficiency using the Kruskal-Wallis rank sum test (Collins & Walling, 2004). Here, any properties returning a statistical significance of $P > 0.05$ were excluded. Properties passing the Kruskal-Wallis test were used in a stepwise discriminant function analysis (DFA) to identify a final composite set of signatures for un-mixing modelling. The estimation of the relative contribution of each potential sediment source to the target time-integrated suspended sediment samples was assessed with the concentration-dependent MixSIAR model (Upadhayay et al., 2018). This model has been widely used for un-mixing compound-specific stable isotopes of odd long-chain n-alkanes (C_{23}-C_{33}). MixSIAR was implemented in the R package linked to the JAGS 3.3.0 library for Bayesian data analysis using a Gibbs sampling Markov chain Monte Carlo (MCMC) algorithm and a fractionation factor of zero was used. The Markov Chain Monte Carlo (MCMC) parameters in the MixSIAR were set as follows: number of chains = 3, chain length = 5,000,000 (extreme), burn = 1,500,000, thin = 500. The convergence of un-mixing models was evaluated using the Gelman-Rubin diagnostic, rejecting the model output if any variable was above 1, in which case the chain length was increased. A diagnostic matrix plot of posterior source contributions was used to evaluate the quality of source discrimination. Density plots of the proportional source contributions are reported along with a mean, median and standard deviation. MixSIAR simulations were run by considering different levels of prior informativeness defined as the sum of the prior input into the model. The input priors ranged from low informative priors in which the sum of the priors input was 1, medium informative priors in which the weight of the prior was set as the number of sources, to very informative priors in which the sum of the priors correspond to 100.

3. Results

3.1. Biomarker signatures among particle size fractions and through time

Source materials collected from paddy fields exhibited the highest n-alkane content (4863.8 ± 1116.2 ng/g in the <25 μm fraction and 5855.9 ± 2294.3 ng/g in the 25–63 μm faction), followed by those from citrus orchards (5513.5 ± 3137.8 ng/g in the <25 μm fraction and 3999.8 ± 1241.4 ng/g in the 25–63 μm fraction), while dry croplands displayed the lowest n-alkane content (2122.5 ± 793.6 ng/g in the 0–25 μm fraction and 2447.5 ± 1506.3 ng/g in the 25–63 μm fraction). N-alkane contents were higher in the finer particle size fractions from citrus orchards, but the trend was reversed for those from paddy fields and dry croplands (Fig. 3). All soil samples showed obvious odd-

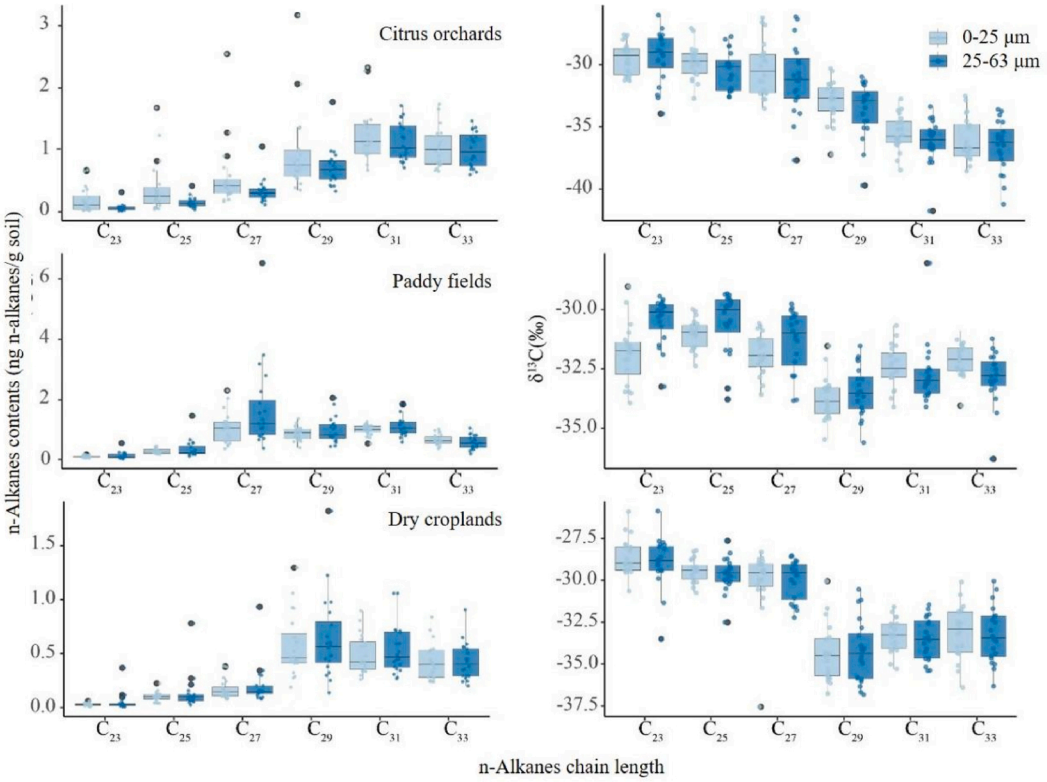

Fig. 3. The biomarker results for the different absolute particle size fractions of the potential sediment sources.

number n-alkane predominance, wherein the dominant peaks were C_{31}, C_{33} and C_{29} in citrus orchard soils, C_{27}, C_{31} and C_{29} in paddy fields soils, and C_{29}, C_{31} and C_{33} in dry cropland soils. These three n-alkanes accounted for more than 60 % of the total n-alkanes. T test was employed to examine the differences in content and $\delta^{13}C$ of n-alkanes between the two particle size fractions. Comparisons revealed some statistically significant differences for soils from paddy fields and citrus orchards (Table 2). On this basis, the <25 μm fraction was used in fingerprinting to minimize potential particle size effects. Molecular biomarkers are potentially influenced by the conversion of organic matter and farming practices through time. We therefore tested for statistically significant differences between the $\delta^{13}C$ of n-alkanes for the two sampling years (Table 3). The results indicated that there were no significant differences and, accordingly, we considered it appropriate to use the soil samples collected from each source in both 2017 and 2018 when estimating the proportional contributions to the target time-integrated suspended sediment.

3.2. Tracer selection and sediment source discrimination

All six fingerprint properties taken forward in the data processing procedure returned a p value of <0.01 from the Kruskal-Wallis H test, with the H-values ranging from 9.59 to 33.52. Individually, the $\delta^{13}C$ of all odd-numbered n-alkanes returned statistically significant differences among the prescribed three sediment source categories (p-value <0.01; Table 4). DFA indicated that the discriminatory efficiency of the individual tracers ranged between 51.7 % and 65.0 %. The $\delta^{13}C_{25}$ was the only individual fingerprint property excluded from the final composite signature set which yielded a discriminatory efficiency of 90 %. On this basis, a final composite signature set combining $\delta^{13}C_{33}$, $\delta^{13}C_{23}$, $\delta^{13}C_{29}$, $\delta^{13}C_{31}$ and $\delta^{13}C_{27}$ was used in MixSIAR to estimate the sources of the time-integrated suspended sediment samples.

3.3. Source contributions to watershed sediment loss

The above results showed that the particle size and organic matter contents have little effect on the carbon isotope contents. The density map of the Bayesian mixing model of carbon isotopes indicates that it can effectively distinguish the various sources of sediment (Fig. 4). The results indicated that for the 12 sediment samples, dry croplands contributed the most (47.4 ± 16.5 %), followed by paddy fields and citrus orchards, which contributed 32.4 ± 14.7 % and 20.2 ± 3.7 % of watershed sediment loss, respectively. There is a slight difference in source contributions between the sampling years, but dry cropland was consistently the most important source for watershed suspended sediment. We analyzed the errors associated with the estimated contributions from each source of sediment and found that the standard deviation varied from 12.7 % to 24.9 %. Here the standard deviation for orchard contributions varied from 12.7 % to 20 %, for paddy fields from 14.3 % to 24.9 %, and for sloping dry cropland from 16.8 % to 23.6 % (Fig. 5).

In 2017, dry croplands contributed 43.4 % of the sampled suspended sediment, whereas paddy fields and citrus orchards accounted for 36.3 % and 20.3 %, respectively. In 2018, dry croplands contributed 53.0 % of sampled sediment, whilst paddy fields and citrus orchards contributed 27.0 % and 20.0 %, respectively. The rice in this area is harvested in late August, and the corresponding contributions of sediment differed before and after the rice harvest. Before the rice harvest, the contribution of the paddy fields was 11.7 % higher (37.3 %) than that after the harvest (25.6 %). After the rice harvest, the sediment contribution from the dry croplands increased by 41.6 % and 55.7 %, respectively. Over the study period, the sediment contributions from the citrus orchards did not

Table 2
T-tests for differences between the content and $\delta^{13}C$ of n-alkanes in two independent particle size fractions (<25 μm and 25–63 μm).

Year	Source categories	Independent-samples T test	δ^{13} of n-alkanes						n-alkanes content										
			$\delta^{13}C_{23}$	$\delta^{13}C_{25}$	$\delta^{13}C_{27}$	$\delta^{13}C_{29}$	$\delta^{13}C_{31}$	$\delta^{13}C_{33}$	C_{23}	C_{24}	C_{25}	C_{26}	C_{27}	C_{28}	C_{29}	C_{30}	C_{31}	C_{32}	C_{33}
2017	Citrus orchards	*F*-value	1.23	0.12	0.04	0.16	0.12	1.56	3.12	0.31	0.03	3.87	0.69	0.09	0.10	0.10	0.05	1.46	0.20
		p-value	0.54	0.25	0.85	0.99	0.33	0.83	0.78	0.46	0.67	0.63	0.98	0.80	0.72	0.74	0.81	0.95	0.58
	Paddy fields	*F*-value	0.16	3.81	0.00	2.67	0.58	0.90	1.57	1.89	1.48	5.49	0.09	1.02	0.67	2.16	6.47	0.78	0.32
		p-value	0.19	0.51	0.41	0.67	0.57	0.49	0.35	0.40	0.99	0.05[a]	0.16	0.40	0.76	0.63	0.42	0.84	0.51
	Dry croplands	*F*-value	1.32	0.55	1.73	0.03	0.01	0.00	0.60	11.25	0.01	4.97	0.30	1.28	0.91	3.36	0.70	0.00	0.32
		p-value	0.41	0.58	0.79	0.69	0.27	0.54	0.94	0.71	0.53	0.54	0.53	0.71	0.76	0.62	0.75	0.78	0.64
2018	Citrus orchards	*F*-value	2.22	2.47	1.41	1.30	0.25	2.01	14.05	20.96	12.15	15.18	3.88	12.95	3.18	11.82	1.20	1.08	0.34
		p-value	0.96	0.33	0.30	0.22	0.24	0.31	0.01[b]	0.00[b]	0.01[b]	0.00[b]	0.82	0.00[b]	0.14	0.01[b]	0.25	0.17	0.47
	Paddy fields	*F*-value	9.36	3.34	0.64	0.01	1.16	0.92	8.52	9.64	6.36	3.27	6.21	3.52	8.75	12.42	6.36	2.18	2.93
		p-value	0.07	0.06	0.06	0.17	0.39	0.08	0.22	0.31	0.22	0.03[a]	0.09	0.23	0.21	0.17	0.22	0.30	0.11
	Dry croplands	*F*-value	0.02	1.14	0.53	0.08	0.35	0.01	5.81	6.24	4.36	5.23	2.56	7.94	1.41	3.91	2.97	1.90	0.08
		p-value	0.97	0.56	0.86	0.75	0.99	0.92	0.25	0.18	0.36	0.23	0.33	0.13	0.46	0.98	0.38	0.50	0.80

[a] Significant difference at the 95 % confidence level.
[b] Significant difference at the 99 % confidence level.

change significantly, remaining at ~20 %. However, in August when the rice was harvested, paddy fields were the main source of sediment in the study catchment (51.7 %), whilst dry croplands and citrus orchards contributed 26.0 and 22.3 %, respectively. Overall, the results showed a specific pattern: August and October were the peak periods of sediment contributions from paddy fields; September, April and July were the peak periods of sediment delivery from dry croplands, while the contributions from orchards remained comparatively stable throughout the year.

4. Discussion

4.1. Factors affecting the distribution and contents of biomarkers

A waxy layer usually develops on the surface of terrestrial higher plant stems, fruits, petals, and leaves to protect plant cells from ultraviolet rays, fungi, and insects. Among these, the epidermal waxy layer of plant leaves has the highest wax content. The composition of plant leaf wax is highly complex, including long-chain alkanes, alcohols, ketones, acids, and lipids (Eglinton & Hamilton, 1967). Plants synthesize organic matter by absorbing water and CO_2 from the environment, and complex isotope fractionation occurs during biosynthesis. Specifically, plants absorb CO_2 from the atmosphere and soil, which leads to differences in the carbon isotopes of organic matter produced by plants with different photosynthetic pathways (Tipple & Pagani, 2007). Isotope fractionation is independent of the organic matter content itself but is influenced by the plant species and environmental factors. The individual carbon isotope ratios of n-alkanes have been widely used to distinguish between vegetation with different photosynthetic pathways (C_3/C_4 plants) (Sun et al., 2016). Notably, the carbon isotope ratios of n-alkanes produced by plants with different pathways show distinct distributions. The $\delta^{13}C$ values of n-alkanes are commonly used to track the relative abundance of C_3 and C_4 vegetation in a given study area. Furthermore, the carbon isotopes of n-alkanes can serve as a tool to explore environmental conditions such as temperature and humidity changes during plant growth. Previous studies have shown that the carbon isotope values of waxes in C_3 plants are closely related to the water supply during photosynthesis (Kohn, 2010; Suh & Diefendorf, 2018; Wang et al., 2018), whereas the correlation between carbon isotope changes and water availability in C_4 plants is less pronounced. In our study, citrus and rice are C_3 vegetation, while corn represents C_4 vegetation. As expected, the n-alkane monomer carbon isotopes of citrus and rice differ due to species-related differences. Consistent with previous studies (Bi et al., 2005; Chikaraishi & Naraoka, 2003; Meyers, 2003), we found that the carbon isotope values of n-alkanes from C_4 plants (corn) are higher than those from C_3 plants. This is confirmed by our results, where dry cropland showed the highest carbon isotope ratio, followed by paddy fields, and then citrus orchards.

Regarding the compound-specific $\delta^{13}C$ of n-alkanes, no significant differences were observed between the two particle size fractions (0–25 μm and 25–63 μm) or across the entire sampling period. This suggests that the monomer carbon isotope of n-alkanes is a reliable sediment fingerprint across different particle size fractions. The lack of significant variation in the δ13C values between the particle size fractions can be explained by the fact that most of the organic carbon is stored in microaggregates (Wang et al., 2017), with the organic matter forms differing between different particle size fractions. For example, the >20 μm fraction is predominantly composed of plant detritus, which decomposes more slowly, and these components are easier to identify in coarse particles than in fine ones. On the other hand, the organic components in the <20 μm fraction mainly consist of

Table 3
T-tests for difference between the $\delta^{13}C$ of n-alkaness in the <25 μm particle size fraction measured in the source categories. i

Source categories	Independent-samples T test	Compound-specific $\delta^{13}C$					
		$\delta^{13}C_{23}$	$\delta^{13}C_{25}$	$C^{13}C_{27}$	$\delta^{13}C_{29}$	$\delta^{13}C_{31}$	$\delta^{13}C_{33}$
Citrus orchards	*F*-value	0.569	0.529	0.213	0.192	0.062	0.579
	p-value	0.108	0.201	0.256	0.364	0.055	0.066
Paddy fields	*F*-value	0.613	0.564	1.418	3.046	0.612	0.019
	p-value	0.241	0.063	0.064	0.133	0.068	0.197
Dry croplands	*F*-value	13.100	26.298	9.151	1.033	0.081	0.321
	p-value	0.322	0.987	0.348	0.061	0.405	0.277

Table 4
Kruskal–Wallis one-way analysis of variance and discrimination function analysis (DFA) for sediment source discrimination.

Fingerprint properties	Kruskal Wallis		Minimization of Wilks' lambda				
	H-value	*p*-value	Step	Wilks' lambda	*F*-value	% source samples classified correctly using individual fingerprint properties	Cumulative % of source samples classified correctly
$\delta^{13}C_{33}$	31.91	0.000[a]	1	0.419	39.57	63.3	63.3
$\delta^{13}C_{23}$	33.52	0.000[a]	2	0.158	42.47	53.3	83.3
$\delta^{13}C_{29}$	9.59	0.008[a]	3	0.102	39.05	51.7	88.3
$\delta^{13}C_{31}$	33.12	0.000[a]	4	0.089	31.70	65.0	90.0
$\delta^{13}C_{27}$	17.31	0.000[a]	5	0.075	28.08	51.7	90.0
$\delta^{13}C_{25}$	25.22	0.000[a]	–	–	–	–	–

"-" indicates fingerprinting properties excluded from the final composite signature.
[a] Significant difference at the 99 % confidence level.

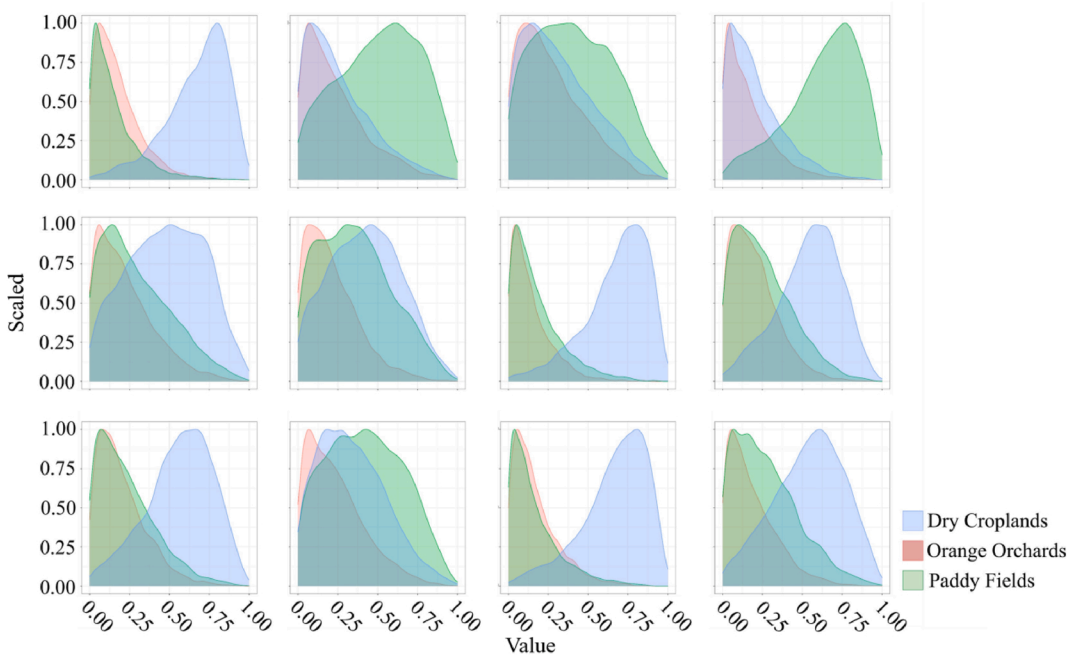

Fig. 4. Density plots of the Bayesian mixture model for carbon isotopes.

sapropelized materials, which have longer transformation times (Baldock & Skjemstad, 2000; Feller & Beare, 1997). Additionally, fine sediments have a larger specific surface area, which allows for more organic matter adsorption.

Our findings suggest that dry cropland is particularly prone to rill erosion, which has poor particle size selectivity, resulting in both coarse and fine particles being transported together with runoff (Shi et al., 2012; Wang et al., 2017). Soil erosion processes can significantly influence the distribution of organic carbon in sediments by redistributing sediment particles of different sizes (Nadeu et al., 2011). Soil erosion selectively delivers finer sediment particles (<25 μm) to the channel, which could reflect the intensity of soil erosion. Additionally, fine particles are more easily transported in paddy fields, while coarser particles mobilized from upstream are more likely to deposit. This particle-size selectivity could explain why fine sediments from paddy fields contribute more to sampled suspended sediment during periods of high erosion. Although these findings do not conclusively prove that individual biomarkers cannot be used as fingerprints, they suggest that the lack of significant differences between particle size

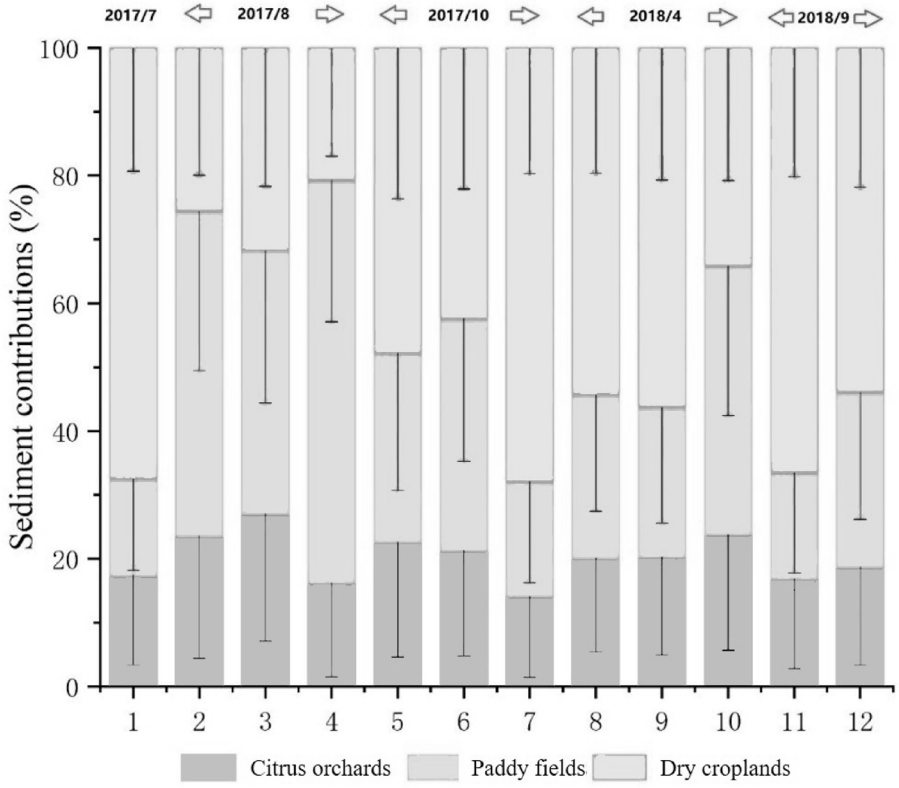

Fig. 5. Source contributions to watershed sediment loss during 2017 and 2018. The error bars indicate the standard deviations (SD).

fractions may be due to the study not analyzing the content of biomarkers in each individual fraction. In regions with relatively stable farming systems and land use, biomarkers remain a reliable tool for sediment source fingerprinting (Chen et al., 2016; Galoski et al., 2019; Hancock & Revill, 2013).

4.2. Land use effects on sediment source contributions

Here we identified principal sediment sources for watershed suspended sediment yields and explored how they contribute to suspended sediment throughout the year. Our research results confirm that cultivated hillslopes is a key source of sediment, which is consistent with previous studies. However, we further emphasized the unique role of rice paddies, which serve as both temporary sediment sinks and secondary sources of sediment during storm events, particularly in the early stages of the growing season. These results emphasize the importance of considering land use and seasonal factors when understanding sediment dynamics in agricultural landscapes. Our findings do not conflict with conventional knowledge that dry croplands can often be a principal sediment source. But our results do highlight the dual roles that paddy fields play in that they act either as a temporary sediment sink along the delivery continuum or as a secondary proximal suspended sediment source. Paddy fields therefore trap freshly eroded sediment carried by storm runoff, whilst also releasing sediment which is transported to the catchment outlet. By way of comparison, in the Wangjiagou catchment, Fuling, paddy field high ridges are sufficient to intercept excess runoff, reduce runoff speed, and reduce the direct impact of raindrops on the field surface soil (Chen et al., 2019). However, in our investigation, we found that from the end of March to the beginning of May, the study catchment is characterized by rice planting. In the initial stage, the paddy fields would be subjected to high-intensity mechanical cultivation, and coarse particles are broken into finer particles. Since the water storage height is minimal, paddy soils are prone to splash erosion after ploughing. When there is runoff, there is a propensity for fine particles of sediment to be mobilized from the paddy fields (Fig. 3). Therefore, in April, paddy fields contributed a large proportion of sediment, as shown in Fig. 5. Any interannual variability in sediment contributions may be due to the spatial heterogeneity of rainfall and resultant erosion (Renschler et al., 1999; Renschler & Harbor, 2002).

Primary sediment sources are site-specific and vary occasionally with catchment size and sediment connectivity determined by catchment properties. In the Three Gorges Reservoir area, rice is generally harvested at the end of August. Due to technological innovation, rice is harvested by machines in mountainous areas. Even small machines cause greater damage to the surface than traditional farming operations. Coupled with the recycling of rice stalks, the ground is exposed due to the lack of mulch and erosion therefore increases. In the same way, dry croplands, where maize is harvested earlier than rice, contributed the most sediment to the study catchment outlet due to the lack of plant cover and the steeper slopes (Chen et al., 2019). Citrus orchards also contributed to suspended sediment loss. As labour costs increase, farmers generally spray herbicides on the ground to kill ground weeds in the orchards to reduce nutrient competition. Despite this, the orchard trees still provide some surface cover, which reduces the splash erosion by raindrops and sediment transport by surface runoff to a certain extent. Here, the retention of the citrus canopy reduces the kinetic energy of raindrops, which is also an important factor in reducing sediment mobilization from the citrus orchards. Monthly sediment contributions from the three sources were also different, which is related to seasonal rainfall, plant growth cycles

and human activities. For example, the rice grows well in July, and the dry cropland has already been harvested, meaning that dry farmland soils contributed the most in July, followed by September and October, due to obvious human activities. In April, the plum rain season has just started, and the early rainfall intensity is not high, meaning that only the finest grain size fraction of sediment is transported. When September comes, the rape planting season begins, and dry croplands and paddy fields are ploughed to sow rape. Bare topsoil, seedlings and mechanical tilling provide ideal conditions for soil erosion in the study catchment currently. Fortunately, after September, the Three Gorges Reservoir area enters the dry season, and the rainfall intensity and amounts are not as severe as during the rainy season.

4.3. Informative options for soil conservation and sediment management

Increasing attention has been directed to environmental challenges posed by intensive crop farming on cultivated hillslopes in the Three Gorges Reservoir Area. Here, the short-distance connectivity for inflowing sediment and associated diffuse pollutants poses a large threat to water quality and ecosystem health of the receiving waters impounded by the reservoir (Fu et al., 2010; Li et al., 2013; Xu et al., 2013; Zhang & Lou, 2011). Farming has been extended to marginal hillslopes and the cultivation intensity has been intensified over the post-dam period. The sustainability of the local community therefore requires precision land use planning and refined conservation schemes to temper the conflicts between ecosystem conservation and rural livelihood improvement when limited land resource is available. According to the 2019 Yangtze River Sediment Bulletin and Chinese national dynamic monitoring of soil erosion, since the reservoir was put into operation in June 2003, the reservoir has accumulated 1.83 billion tons of silt. In 2018, the area of soil erosion in the Three Gorges Reservoir area was 19,200 km^2, accounting for 33.34 % of land. Eutrophication has been a serious problem, and the tributaries are frequently subjected to algal blooms. The statistical evaluation of 649 groups of data from 28 tributaries from 2004 to 2007 shows that the proportion of tributaries suffering light eutrophication is 75 % (Wang & Qian, 2009). One of the most important reasons for this is that the sediment in the agricultural catchment surrounding the reservoir area is directly delivered into the Yangtze River.

Small watersheds are the basic unit of sediment yield, sediment transport and soil erosion control. Carrying out comprehensive management of water and soil erosion in small watersheds is critical in reducing the inflow of sediment, improving the ecological environment, and maximizing reservoir life span. In order to reduce soil erosion in agricultural catchments, the farming system should be optimized based on increasing the implementation of water and soil conservation measures, such as the promotion of soil virginization technology and changing deep tillage to shallow tillage. This can reduce the artificial fragmentation of soil aggregates. Soils with many water-stable aggregates are more resistant to the formation of soil crusts, have good infiltration, and have less runoff and erosion (Fox et al., 2004). Especially in the case of paddy fields, the implementation of paddy field soil virginization, which can change the micro-topography, thicken the active soil layer for roots and make the capillary pores of the soil connect normally to improve water and air flow represents an important management intervention. In addition, the strategy of returning straw to the field should be promoted. Returning straw to fields can effectively promote microbial activity which degrades the organic components in the straw, increase soil organic matter, optimize the physical structure of the soil, and improve soil fertility (Hamm et al., 2016; Li et al., 2019; Liu et al., 2014). At the same time, straw mulch can intercept rainfall, prevent water volatilization, and form a natural farmland reservoir. Covering the ground with straw can also effectively reduce rainfall kinetic energy, intercept runoff, and greatly reduce soil erosion (Shi et al., 2013). The technology of returning straw to the fields can also greatly increase soil carbon sequestration and reduce greenhouse gases emitted into the atmosphere. For the citrus orchards, the method of pasture culture is recommended. The specific measures of this intervention are to interplant Leguminosae or Poaceae between the rows of orchards or beneath orchards in their entirety, cut them regularly, cover the underside of the trees with the cut stalks, and allow them to decay and decompose naturally (Richardson, 1986). These actions are designed to improve soil structure and soil fertility and reduce soil erosion. Studies on the Three Gorges Reservoir area show that vetch (*vicia villosa Roth* var.) is an ideal understory vegetation (Wen et al., 2011). In conjunction with this intervention, herbicides are applied in orchards, which protects the environment. At the same time, as a legume, it can not only fix nitrogen, but also increase soil organic matter after decay.

4.4. Model uncertainty analysis

Here we used Bayesian mixing model to quantify the contributions of land use-based sources to watershed sediment loss given its ability to integrate prior information and observational data. However, model uncertainty remains a critical issue, stemming primarily from the choice of prior information, the quality of observational data, and the inherent assumptions in the model. The selection of prior information is one of the core elements of a Bayesian model, but it can significantly influence the model output. Variations in the informativeness of priors can lead to substantial differences in the posterior distributions (Lizaga et al., 2021). In this study, we adopted uninformative priors to minimize the influence of subjective assumptions on model outcomes (Lizaga et al., 2022, 2024). However, uninformative priors have limitations, such as potentially increasing the uncertainty of results when the sample size is small. Future studies could consider integrating weakly informative priors based on regional geological context, sediment characteristics, and existing tracer data distributions. This approach could help balance the reduction of uncertainty with improving model robustness. The quality and characteristics of input data are also critical to the results of the Bayesian model. In this study, we initially compared the use of n-alkane and carbon isotopic data from <25 μm to <63 μm particle size fractions and found no significant differences in model outcomes. This indicates that within the scope of our study, particle size fractionation had a relatively stable impact on source apportionment results. However, other studies have highlighted the sensitivity of posterior results to the choice and distribution of tracers (Gaspar et al., 2022; Upadhayay, Lamichhane, et al., 2020; Wynants et al., 2020). It is therefore essential to carefully evaluate the quality of input data, the representativeness of tracers, and their distinguishability among source areas during model construction. The assumptions underlying the Bayesian mixing model also warrant consideration. These models often assume that tracers follow a normal distribution and that source contributions follow prior distributions. However, these assumptions may not always reflect actual conditions, as tracer distributions may exhibit skewness or multimodal characteristics. Such discrepancies could result in model outcomes that deviate from reality. Future research could integrate alternative approaches, such as Monte Carlo simulations or machine learning techniques, to validate or refine these assumptions, thereby reducing uncertainty and improving the credibility of the results (Latorre et al., 2025; Yang et al., 2025). In summary, model uncertainty is a key challenge in applying

Bayesian mixing models to sediment source apportionment. This study found that particle size fractionation had a minimal impact on model outcomes, and the use of uninformative priors effectively reduced subjective bias. However, further exploration is needed to optimize prior information, improve input data quality, and refine model assumptions, thereby reducing uncertainty and enhancing the robustness of the results.

4.5. Limitations of this study and future research directions

The mainstream biomarkers employed for source fingerprinting are primarily fatty acids and n-alkanes (Cooper et al., 2015; Gibbs, 2008; Mabit et al., 2018; Reiffarth et al., 2016, 2019; Upadhayay et al., 2018). Compared to fatty acids, n-alkanes are more resistant to decomposition, which makes them a reliable proxy for sediment source tracking. Previous studies have reported the use of n-alkane content for sediment source identification (Chen et al., 2016, 2017), with monomer carbon isotopes of fatty acids and n-alkanes being widely utilized. While decomposition affects the content of total organic matter, the $\delta^{13}C$ isotopic signature of these compounds remains stable. Short-chain fatty acids, such as C16:0 and C18:0, dissolve in water and migrate with it, making them suitable biomarkers for monitoring deep soil erosion, especially in areas prone to tunnel erosion, such as the Loess Plateau (Gibbs, 2008; Zhu, 2012). In contrast, longer-chain fatty acids and n-alkanes, which are water-insoluble, are better suited for areas dominated by surface erosion (Mabit et al., 2018; Reiffarth et al., 2016, 2019; Upadhayay et al., 2018). These differences in solubility and erosion processes highlight the utility of different biomarkers for fingerprinting specific erosion processes.

Our study analyzed the carbon isotopes ($\delta^{13}C$) of n-alkanes. Future research could expand this approach by incorporating $\delta^{2}D$ isotopes and extending the analysis to fatty acids. If fatty acids are used as fingerprints, the three CHO isotopes ($\delta^{13}C$, $\delta^{2}D$, and $\delta^{18}O$) could also be tested to provide more comprehensive insights into sediment source contributions. A challenge in fingerprinting lies in the limitations of existing models. Most fingerprinting models provide an optimal solution; however, the solution set interval for these methods is often too narrow. As a result, an optimal or approximate solution may only represent one of many possible sediment source contribution scenarios in a catchment (Chen et al., 2017; Collins et al., 1997, 2010). The complex interplay between surface soils, land use, rainfall, and hydrology further complicate this issue, as the same magnitude of sediment loss can arise from varying source contributions—commonly referred to as the "black box" model of soil erosion (Borrelli et al., 2021). To address this, the MixSIAR model was applied, which treats the solution space as a normal distribution and accounts for the likelihood of extreme sediment source contributions. Unlike traditional models, MixSIAR does not overly constrain sediment source contributions, thus providing a more realistic reflection of actual conditions (Garzon-Garcia et al., 2017; Parnell et al., 2010; Xue et al., 2009). However, absolute source contributions for the study catchment, including paddy fields, were not calculated due to the absence of suspended sediment load monitoring data.

5. Conclusion

Our study examined the behaviour of biomarkers (both absolute abundance and compound-specific stable isotopes of n-alkanes) and variability among different particle size fractions. Target time-integrated suspended sediments collected at the watershed outlet were further apportioned to land use-based source categories in a fragmented landscape with intensive farming practices. The absolute abundance of n-alkanes (C_{23}-C_{33}) in surface soils, especially of paddy fields, displayed obvious seasonal difference, which is probably related to farming practices, plant growth dynamics and the redox environment involved. This implies the necessity to undertake repeat sampling to improve the temporal representativeness of sample collection when using organic tracers. However, compound-specific $\delta^{13}C$ of n-alkanes exhibited no significant seasonal or particle size-related variability, thereby providing a reliable conservative tracer. Sediment fingerprinting with compound-specific $\delta_{13}C$ of n-alkanes highlighted the relative importance of paddy fields as a temporary secondary sediment source to watershed sediment loss, especially during the early spring when ploughing and rice planting are usually performed. Traditionally regarded as sediment sinks due to the influx of turbid irrigation runoff, paddy fields were found to contribute significant amounts of suspended sediment, especially before rice establishment when soil disturbance is high. Soil conservation and sediment management measures need to target principal soil erosion and sediment delivery processes with larger contributions to watershed sediment loss.

CRediT authorship contribution statement

Qiang Tang: Writing – review & editing, Writing – original draft, Visualization, Validation, Methodology, Investigation, Funding acquisition, Conceptualization. **Fangxin Chen:** Writing – review & editing, Writing – original draft, Visualization, Validation, Methodology, Investigation. **Guangyu Zhu:** Investigation, Formal analysis. **Xiubin He:** Writing – review & editing, Conceptualization. **Jie Wei:** Writing – review & editing. **Yusheng Zhang:** Writing – review & editing, Formal analysis. **Hari Ram Upadhayay** Writing – original draft, Resources, Methodology. **Adrian Joynes:** Writing – original draft, Methodology, Data curation. **Adrian L. Collins:** Writing – review & editing, Supervision, Investigation, Funding acquisition, Conceptualization.

Declaration of competing interest

The authors declare that they have no conflict of interest.

Acknowledgements

This work was supported by the National Key Research and Development Program of China (2023YFF1305203), the National Natural Science Foundation of China (42477340), the Royal Society Newton International Fellowship (NF161415) awarded to Qiang Tang and supervised by Adrian Collins, the Newton International Fellowships Alumni (AL\231030), and the Special Fund for Youth Team of Southwest University (SWU-XDJH-202306). The contribution by Adrian Collins was also funded by the UK Research and Innovation–Biotechnology and Biological Sciences Research Council (UKRI-BBSRC) via grant award BB/X010961/1 (Resilient Farming Futures) – specifically work package 2 - BBS/E/RH/230004B; Detecting agroecosystem 'resilience' using novel data science methods.

References

Apitz, S. E. (2012). Conceptualizing the role of sediment in sustaining ecosystem services: Sediment-ecosystem regional assessment (SEcoRA). *Science of the Total Environment, 415*, 9–30.

Baldock, J. A., & Skjemstad, J. O. (2000). Role of the soil matrix and minerals in protecting natural organic materials against biological attack. *Organic Geochemistry, 31*(7), 697–710.

Ben Slimane, A., Raclot, D., Evrard, O., Sanaa, M., Lefevre, I., Ahmadi, M., … Le Bissonnais, Y. (2013). Fingerprinting sediment sources in the outlet reservoir of a hilly cultivated catchment in Tunisia. *Journal of Soils and Sediments, 13*(4), 801–815.

Bi, X., Sheng, G., Liu, X., Li, C., & Fu, J. (2005). Molecular and carbon and hydrogen isotopic composition of n-alkanes in plant leaf waxes. *Organic Geochemistry, 36*(10), 1405–1417.
Blake, W. H., Ficken, K. J., Taylor, P., Russell, M. A., & Walling, D. E. (2012). Tracing crop-specific sediment sources in agricultural catchments. *Geomorphology, 139*, 322–329.
Borrelli, P., Alewell, C., Alvarez, P., Annache, J. A. A., Baartman, J., Ballabio, C., … Panagos, P. (2021). Soil erosion modelling: A global review and statistical analysis. *Science of the Total Environment, 780*, Article 146494.
Borrelli, P., Robinson, D. A., Panagos, P., Lugato, E., Yang, J. D., Alewell, C., … Ballabio, C. (2020). Land use and climate change impacts on global soil erosion by water (2015-2070). *Proceedings of the National Academy of Sciences of the United States of America, 117*(36), 21994–22001.
Chen, F. X., Fang, N. F., & Shi, Z. H. (2016). Using biomarkers as fingerprint properties to identify sediment sources in a small catchment. *Science of the Total Environment, 557*, 123–133.
Chen, F. X., Fang, N. F., Wang, Y. X., Tong, L. S., & Shi, Z. H. (2017). Biomarkers in sedimentary sequences: Indicators to track sediment sources over decadal timescales. *Geomorphology, 278*, 1–11.
Chen, F. X., Wang, X. Y., Li, X. X., Wangm, J. L., Xie, D. T., Ni, J. P., & Liu, Y. J. (2019). Using the sediment fingerprinting method to identify the sediment sources in small catchments with similar geological conditions. *Agriculture, Ecosystems & Environment, 286*, Article 106655.
Chikaraishi, Y., & Naraoka, H. (2003). Compound-specific δ^2D–$\delta^{13}C$ analyses of n-alkanes extracted from terrestrial and aquatic plants. *Phytochemistry, 63*(3), 361–371.
Collins, A. L., Burak, E., Harris, P., Pelley, S., Cardenas, L., & Tang, Q. (2019). Field scale temporal and spatial variability of delta C-13, delta N-15., TC and TN soil properties: Implications for sediment source tracing. *Geoderma, 333*, 108–122.
Collins, A. L., Pulley, S., Foster, I. D. L., Gellis, A., Porto, P., & Horowitz, A. J. (2017). Sediment source fingerprinting as an aid to catchment management: A review of the current state of knowledge and a methodological decision-tree for end-users. *Journal of Environmental Management, 194*, 86–108.
Collins, A. L., & Walling, D. E. (2004). Documenting catchment suspended sediment sources: Problems, approaches and prospects. *Progress in Physical Geography, 28*(2), 159–196.
Collins, A., Walling, D., & Leeks, G. (1997). Source type ascription for fluvial suspended sediment based on a quantitative composite fingerprinting technique. *Catena, 29*(1), 1–27.
Collins, A. L., Walling, D. E., Webb, L., & King, P. (2010). Apportioning catchment scale sediment sources using a modified composite fingerprinting technique incorporating property weightings and prior information. *Geoderma, 155*(3–4), 249–261.
Cooper, R. J., Pedentchouk, N., Hiscock, K. M., Disdle, P., Krueger, T., & Rawlins, B. G. (2015). Apportioning sources of organic matter in streambed sediments: An integrated molecular and compound-specific stable isotope approach. *Science of the Total Environment, 520*, 187–197.
Du, P. F., & Walling, D. E. (2017). Fingerprinting surficial sediment sources: Exploring some potential problems associated with the spatial variability of source material properties. *Journal of Environmental Management, 194*, 4–15.
Eglinton, G., & Hamilton, R. J. (1967). Leaf epicuticular waxes. *Science, 156*(3780), 1322–1335.
Fang, H. Y. (2015). Temporal variations of sediment source from a reservoir catchment in the black soil region, Northeast China. *Soil and Tillage Research, 153*, 59–65.
Feller, C., & Beare, M. H. (1997). Physical control of soil organic matter dynamics in the tropics. *Geoderma, 79*(1), 69–116.
Fox, D. M., Bryan, R. B., & Fox, C. A. (2004). Changes in pore characteristics with depth for structural crusts. *Geoderma, 120*(1), 109–120.
Fox, J. F., & Papanicolaou, A. N. (2008). Application of the spatial distribution of nitrogen stable isotopes for sediment tracing at the watershed scale. *Journal of Hydrology, 358*(1–2), 46–55.
Fu, B. J., Wu, B. F., Lu, Y. H., Xu, Z. H., Cao, J. H., Niu, D., … Zhou, Y. M. (2010). Three Gorges project: Efforts and challenges for the environment. *Progress in Physical Geography, 34*(6), 741–754.
Galoski, C. E., Jiménez Martínez, A. E., Schultz, G. B., dos Santos, I., & Froehner, S. (2019). Use of n-alkanes to trace erosion and main sources of sediments in a watershed in southern Brazil. *Science of the Total Environment, 682*, 447–456.
Garzon-Garcia, A., Laceby, J. P., Olley, J. M., & Bunn, S. E. (2017). Differentiating the sources of fine sediment, organic matter and nitrogen in a subtropical Australian catchment. *Science of the Total Environment, 575*, 1384–1394.
Gaspar, L., Blake, W. H., Lizaga, I., Latorre, B., & Navas, A. (2022). Particle size effect on geochemical composition of experimental soil mixtures relevant for unmixing modelling. *Geomorphology, 403*, Article 108178.
Gibbs, M. M. (2008). Identifying source soils in contemporary estuarine sediments: A new compound-specific isotope method. *Estuary Coast, 31*(2), 344–359.
Hamm, A. C., Tenuta, M., Krause, D. O., Ominski, K. H., Tkachuk, V. L., & Flaten, D. N. (2016). Bacterial communities of an agricultural soil amended with solid pig and dairy manures, and urea fertilizer. *Applied Soil Ecology, 103*, 61–71.
Hancock, G. J., & Revill, A. T. (2013). Erosion source discrimination in a rural Australian catchment using compound-specific isotope analysis (CSIA). *Hydrological Processes, 27*(6), 923–932.
He, X. B., Bao, Y. H., Nan, H. W., Xiong, D. H., Wang, L., Liu, Y. F., & Zhao, J. B. (2009). Tillage pedogenesis of purple soils in southwestern China. *Journal of Mountain Science, 6*(2), 205–210.
Huang, D. H., Du, P. F., Wang, J., Wei, X., Liu, B., & Xu, J. J. (2019). Using reservoir deposits to quantify the source contributions to the sediment yield in the Black Soil Region, Northeast China, based on the fingerprinting technique. *Geomorphology, 339*, 1–18.
Jenny, J. P., Koirala, S., Gregory-Eaves, I., Francus, P., Niemann, C., Ahrens, B., … Carvalhais, N. (2019). Human and climate global-scale imprint on sediment transfer during the Holocene. *Proceedings of the National Academy of Sciences of the United States of America, 116*(46), 22972–22976.
Kayvantash, D., Cojan, I., Kissel, C., & Franke, C. (2017). Magnetic fingerprint of the sediment load in a meander bend section of the Seine River (France). *Geomorphology, 286*, 14–26.
Kim, J. K., Onda, Y., Yang, D. Y., & Kim, M. S. (2013). Temporal variations of reservoir sediment sources in a small mountainous catchment in Korea. *Earth Surface Processes and Landforms, 38*(12), 1380–1392.
Kohn, M. J. (2010). Carbon isotope compositions of terrestrial C3 plants as indicators of (paleo)ecology and (paleo)climate. *Proceedings of the National Academy of Sciences of the United States of America, 107*(46), 19691–19695.
Latorre, B., Lizaga, I., Gaspar, L., & Navas, A. (2025). Evaluating the impacts of high source variability and extreme contributing sources on sediment fingerprinting models. *Water Resources Management*. https://doi.org/10.1007/s11269-025-04169-8
Li, X. B., He, X. B., Zhang, X. D., Yan, X. Y., Six, J., Cai, Z. C., … Li, Z. A. (2019). Distinct responses of soil fungal and bacterial nitrate immobilization to land conversion from forest to agriculture. *Soil Biology and Biochemistry, 134*, 81–89.
Li, K. F., Zhu, C., Wu, L., & Huang, L. Y. (2013). Problems caused by the three Gorges dam construction in the Yangtze River basin: A review. *Environmental Reviews, 21*(3), 127–135.
Liu, C., Lu, M., Cui, J., Li, B., & Fang, C. M. (2014). Effects of straw carbon input on carbon dynamics in agricultural soils: A meta-analysis. *Global Change Biology, 20*(5), 1366–1381.
Lizaga, I., Bodé, S., Gaspar, L., Latorre, B., Boeckx, P., & Navas, A. (2021). Legacy of historic land cover changes on sediment provenance tracked with isotopic tracers in a Mediterranean agroforestry catchment. *Journal of Environmental Management, 288*, Article 112291.
Lizaga, I., Latorre, B., Bodé, S., Gaspar, L., Boeckx, P., & Navas, A. (2024). Combining isotopic and elemental tracers for enhanced sediment source partitioning in complex catchments. *Journal of Hydrology, 631*, Article 130768.
Lizaga, I., Latorre, B., Gaspar, L., & Navas, A. (2022). Combined use of geochemistry and compound-specific stable isotopes for sediment fingerprinting and tracing. *Science of the Total Environment, 832*, Article 154834.
Ludwig, W., Probst, J. L., & Kempe, S. (1996). Predicting the oceanic input of organic carbon by continental erosion. *Global Biogeochemical Cycles, 10*(1), 23–41.
Mabit, L., Gibbs, M., Mbaye, M., Meusburger, K., Toloza, A., Resch, C., … Alewell, C. (2018). Novel application of Compound Specific Stable Isotope (CSSI) techniques to investigate on-site sediment origins across arable fields. *Geoderma, 316*, 19–26.
Martinez-Carreras, N., Krein, A., Gallart, F., Iffly, J. F., Pfister, L., Hoffmann, L., & Owens, P. N. (2010). Assessment of different colour parameters for discriminating potential suspended sediment sources and provenance: A multi-scale study in Luxembourg. *Geomorphology, 118*(1–2), 118–129.
Meyers, P. A. (2003). Applications of organic geochemistry to paleolimnological reconstructions: A summary of examples from the laurentian great lakes. *Organic Geochemistry, 34*(2), 261–289.
Nadeu, E., de Vente, J., Martínez-Mena, M., & Boix-Fayos, C. (2011). Exploring particle size distribution and organic carbon pools mobilized by different erosion processes at the catchment scale. *Journal of Soils and Sediments, 11*(4), 667–678.
Owens, P. N., Walling, D. E., & Leeks, G. J. L. (1999). Use of floodplain sediment cores to investigate recent historical changes in overbank sedimentation rates and sediment sources in the catchment of the River Ouse, Yorkshire, UK. *Catena, 36*(1–2), 21–47.
Parnell, A. C., Inger, R., Bearhop, S., & Jackson, A. L. (2010). Source partitioning using stable isotopes: Coping with too much variation. *PLoS One, 5*(3), Article e9672.
Phillips, J. M., Russell, M. A., & Walling, D. E. (2000). Time-integrated sampling of fluvial suspended sediment: A simple methodology for small catchments. *Hydrological Processes, 14*(14), 2589–2602.
Pulley, S., Foster, I., & Collins, A. L. (2017). The impact of catchment source group classification on the accuracy of sediment fingerprinting outputs. *Journal of Environmental Management, 194*, 16–26.
Pulley, S., Goubet, A., Moser, I., Browning, S., & Collins, A. L. (2019). The sources and dynamics of fine-grained sediment degrading the Freshwater Pearl Mussel (Margaritifera margaritifera) beds of the River Torridge, Devon, UK. *Science of the Total Environment, 657*, 420–434.
Pulley, S., Van der Waal, B., Rowntree, K., & Collins, A. L. (2018). Colour as reliable tracer to identify the sources of historically deposited flood bench sediment in the Transkei, South Africa: A comparison with mineral magnetic tracers before and after hydrogen peroxide pre-treatment. *Catena, 160*, 242–251.
Reiffarth, D. G., Petticrew, E. L., Owens, P. N., & Lobb, D. A. (2016). Sources of variability in fatty acid (FA) biomarkers in the application of compound-specific stable isotopes (CSSIs) to soil and sediment fingerprinting and tracing: A review. *Science of the Total Environment, 565*, 8–27.
Reiffarth, D. G., Petticrew, E. L., Owens, P. N., & Lobb, D. A. (2019). Spatial differentiation of cultivated soils using compound-specific stable isotopes (CSSIs) in a temperate agricultural watershed in Manitoba, Canada. *Journal of Soils and Sediments, 19*(9), 3411–3426.

Renschler, C. S., & Harbor, J. (2002). Soil erosion assessment tools from point to regional scales-the role of geomorphologists in land management research and implementation. *Geomorphology, 47*(2), 189–209.
Renschler, C., Mannaerts, C., & Diekkrüger, B. (1999). Evaluating spatial and temporal variability in soil erosion risk—rainfall erosivity and soil loss ratios in Andalusia, Spain. *Catena, 34*(3), 209–225.
Richardson, A. (1986). The effects of herbicide soil management systems and nitrogen fertilizer on the eating quality of Cox's Orange Pippin apples. *Journal of Horticultural Science, 61*(4), 447–456.
Rowntree, K. M., van der Waal, B. W., & Pulley, S. (2017). Magnetic susceptibility as a simple tracer for fluvial sediment source ascription during storm events. *Journal of Environmental Management, 194*, 54–62.
Shi, Z. H., Fang, N. F., Wu, F. Z., Wang, L., Yue, B. J., & Wu, G. L. (2012). Soil erosion processes and sediment sorting associated with transport mechanisms on steep slopes. *Journal of Hydrology, 454*, 123–130.
Shi, Z. H., Yue, B. J., Wang, L., Fang, N. F., Wang, D., & Wu, F. Z. (2013). Effects of mulch cover rate on Interrill erosion processes and the size selectivity of eroded sediment on steep slopes. *Soil Science Society of America Journal, 77*(1), 257–267.
Suh, Y. J., & Diefendorf, A. F. (2018). Seasonal and canopy height variation in n-alkanes and their carbon isotopes in a temperate forest. *Organic Geochemistry, 116*, 23–34.
Sun, Q., Xie, M. M., Lin, Y., Shan, Y. B., Zhu, Q. Z., Xu, D. K., … Chu, G. Q. (2016). An n-alkane and carbon isotope record during the last deglaciation from annually laminated sediment in Lake Xiaolongwan, northeastern China. *Journal of Paleolimnology, 56*(2), 189–203.
Tang, Q., Fu, B. J., Wen, A. B., Zhang, X. B., He, X. B., & Collins, A. L. (2019). Fingerprinting the sources of water-mobilized sediment threatening agricultural and water resource sustainability: Progress, challenges and prospects in China. *Science China Earth Sciences, 62*, 2017–2030, 2019.
Theuring, P., Collins, A. L., & Rode, M. (2015). Source identification of fine-grained suspended sediment in the Kharaa River basin, northern Mongolia. *Science of the Total Environment, 526*, 77–87.
Tiecher, T., Caner, L., Minella, J. P. G., Bender, M. A., & dos Santos, D. R. (2016). Tracing sediment sources in a subtropical rural catchment of southern Brazil by using geochemical tracers and near-infrared spectroscopy. *Soil and Tillage Research, 155*, 478–491.
Tipple, B. J., & Pagani, M. (2007). The early origins of terrestrial C4 photosynthesis. *Annual Review of Earth and Planetary Sciences, 35*(1), 435–461.
Upadhayay, H. R., Bode, S., Griepentrog, M., Huygens, D., Bajracharya, R. M., Blake, W. H., … Boeckx, P. (2017). Methodological perspectives on the application of compound-specific stable isotope fingerprinting for sediment source apportionment. *Journal of Soils and Sediments, 17*(6), 1537–1553.
Upadhayay, H. R., Griepentrog, M., Bode, S., Bajracharya, R. M., Cornelis, W., Collins, A. L., & Boeckx, P. (2020). Catchment-wide variations and biogeochemical time lags in soil fatty acid carbon isotope composition for different land uses: Implications for sediment source classification. *Organic Geochemistry, 146*, Article 104048.
Upadhayay, H. R., Lamichhane, S., Bajracharya, R. M., Cornelis, W., Collins, A. L., & Boeckx, P. (2020). Sensitivity of source apportionment predicted by a Bayesian tracer mixing model to the inclusion of a sediment connectivity index as an informative prior: Illustration using the Kharka catchment (Nepal). *Science of the Total Environment, 713*, Article 136703.
Upadhayay, H. R., Smith, H. G., Griepentrog, M., Bode, S., Bajracharya, R. M., Blake, W., … Boeckx, P. (2018). Community managed forests dominate the catchment sediment cascade in the mid-hills of Nepal: A compound-specific stable isotope analysis. *Science of the Total Environment, 637*, 306–317.
Vercruysse, K., & Grabowski, R. C. (2018). Using source-specific models to test the impact of sediment source classification on sediment fingerprinting. *Hydrological Processes, 32*(22), 3402–3415.
Verheyen, D., Diels, J., Kissi, E., & Poesen, J. (2014). The use of visible and near-infrared reflectance measurements for identifying the source of suspended sediment in rivers and comparison with geochemical fingerprinting. *Journal of Soils and Sediments, 14*(11), 1869–1885.
Walling, D. E. (2006). Human impact on land–ocean sediment transfer by the world's rivers. *Geomorphology, 79*(3–4), 192–216.
Walling, D. E., & Fang, D. (2003). Recent trends in the suspended sediment loads of the world's rivers. *Global and Planetary Change, 39*(1–2), 111–126.
Wang, Y. X., Fang, N. F., Zhang, F. B., Wang, L., Wu, G. L., & Yang, M. Y. (2017). Effects of erosion on the microaggregate organic carbon dynamics in a small catchment of the Loess Plateau, China. *Soil and Tillage Research, 174*, 205–213.
Wang, Z. F., & Qian, Y. F. (2009). Frequency and intensity of extreme precipitation events in China. *Advances in Water Science, 20*(1), 1–9.
Wang, J., Xu, Y. P., Zhou, L. P., Shi, M. R., Axia, E., Jia, Y. F., … Wang, G. A. (2018). Disentangling temperature effects on leaf wax n-alkane traits and carbon isotopic composition from phylogeny and precipitation. *Organic Geochemistry, 126*, 13–22.
Wen, M. X., Shi, X. J., Nie, Z. P., Liu, W. F., & Zhou, X. B. (2011). Effect of summer green manure in Pankan tangerine orchard. *Journal of Fruit Science, 28*(6), 1077–1081.
Wuepper, D., Borrelli, P., & Finger, R. (2020). Countries and the global rate of soil erosion. *Nature Sustainability, 3*(1), 51–55.
Wynants, M., Millward, G., Patrick, A., Taylor, A., Munishi, L., Mtei, K., … Blake, W. H. (2020). Determining tributary sources of increased sedimentation in East-African Rift Lakes. *Science of the Total Environment, 717*, Article 137266.
Xu, X. B., Tan, Y., & Yang, G. S. (2013). Environmental impact assessments of the three Gorges project in China: Issues and interventions. *Earth-Science Reviews, 124*, 115–125.
Xue, D., Botte, J., De Baets, B., Accoe, F., Nestler, A., Taylor, P., … Boecjx, P. (2009). Present limitations and future prospects of stable isotope methods for nitrate source identification in surface- and groundwater. *Water Research, 43*(5), 1159–1170.
Yang, Y., Xu, J., Chen, J., Ye, W., Ran, L., Wang, K., … Chen, F. (2025). Application of mass balance and unmixing model to trace sediment sources in an agricultural catchment. *Catena, 252*, Article 108846.
Zhang, Q. F., & Lou, Z. P. (2011). The environmental changes and mitigation actions in the Three Gorges Reservoir region, China. *Environmental Science & Policy, 14*(8), 1132–1138.
Zhou, H. P., Chang, W. N., & Zhang, L. J. (2016). Sediment sources in a small agricultural catchment: A composite fingerprinting approach based on the selection of potential sources. *Geomorphology, 266*, 11–19.
Zhu, T. X. (2012). Gully and tunnel erosion in the hilly Loess Plateau region, China. *Geomorphology, 153*, 144–155.